NANO LETTERS

Letter

Atomic and Electronic Structure of Graphene-Oxide

K. Andre Mkhoyan, Alexander W. Contryman, John Silcox, Derek A. Stewart, Goki Eda, Cecilia Mattevi, Steve Miller, and Manish Chhowalla

Nano Lett., **2009**, 9 (3), 1058-1063• DOI: 10.1021/nl8034256 • Publication Date (Web): 06 February 2009

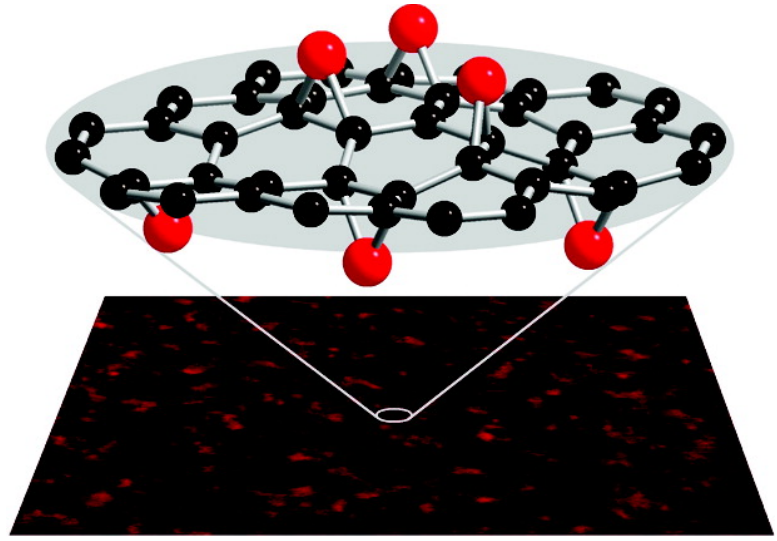

NANO LETTERS

2009
Vol. 9, No. 3
1058-1063

Atomic and Electronic Structure of Graphene-Oxide

K. Andre Mkhoyan,*,†,‡ Alexander W. Contryman,† John Silcox,† Derek A. Stewart,§ Goki Eda,|| Cecilia Mattevi,|| Steve Miller,|| and Manish Chhowalla||

School of Applied and Engineering Physics, Cornell University, Ithaca, New York 14853, Department of Chemical Engineering and Materials Science, University of Minnesota, Minneapolis, Minnesota 55455, Cornell Nanoscale Facility, Cornell University, Ithaca, New York 14853, Department of Material Science and Engineering, Rutgers University, Piscataway, New Jersey 08854

Received November 12, 2008; Revised Manuscript Received January 3, 2009

ABSTRACT

We elucidate the atomic and electronic structure of graphene oxide (GO) using annular dark field imaging of single and multilayer sheets and electron energy loss spectroscopy for measuring the fine structure of C and O K-edges in a scanning transmission electron microscope. Partial density of states and electronic plasma excitations are also measured for these GO sheets showing unusual $\pi^* + \sigma^*$ excitation at 19 eV. The results of this detailed analysis reveal that the GO is rough with an average surface roughness of 0.6 nm and the structure is predominantly amorphous due to distortions from sp^3 C−O bonds. Around 40% sp^3 bonding was found to be present in these sheets with measured O/C ratio of 1:5. These sp^2 to sp^3 bond modifications due to oxidation are also supported by ab initio calculations.

Thin sheets of graphene oxide (GO) have recently emerged as a new carbon-based nanoscale material that also provides an alternative path to graphene.[1−11] The solubility of graphene oxide in water and other solvents allows it to be uniformly deposited onto wide ranging substrates in the form of thin films or networks which makes it potentially useful for macroelectronics.[5−8,10,11] Graphene oxide is an insulator but controlled oxidation provides tunability of the electronic and mechanical properties including the possibility of accessing zero-band gap graphene via complete removal of the C−O bonds. The structure of GO is often simplistically assumed to be a graphene sheet bonded to oxygen in the form of carboxyl, hydroxyl or epoxy groups. In this letter, we elucidate the atomic and electronic structure of GO using composition sensitive annular dark field (ADF) imaging of single and multilayer sheets and electron energy loss spectroscopy (EELS) for measuring the fine structure of the carbon and oxygen K-edges as well as low-loss electronic excitations in a scanning transmission electron microscope (STEM). The results reveal that the GO sheets are rough with an average roughness of 0.6 nm and the structure is predominantly amorphous due to distortions from the high fraction of sp^3 C−O bonds. About 40% sp^3 bonding was found for O/C ratio of 1:5 in these GO films. Our results suggest that chemical removal of oxygen, using hydrazine for example, may leave behind a highly distorted reduced graphene oxide, which is likely to have substantially lower carrier mobilities than pure graphene, as has been observed in several device studies.[6,8,12]

Scanning transmission electron microscopy combined with electron energy loss spectroscopy has proven to be a very effective for measuring electronic and optical properties.[13] A simple and intimate connection between local density of the unoccupied electronic states and the core-level excitations allows direct measurements of both the energy distribution and density of states for the levels above the Fermi energy.[14,15] The low loss region of EELS measures optical properties by recording electronic transitions between critical points of conduction and valence bands as well as characteristic plasmon excitations, which lead to real and imaginary parts of dielectric function of the material.[16] Several TEM observations on graphene and graphene oxide have been reported,[17−21] but a detailed analysis of the atomic and electronic structure for GO has been lacking. Cai et al. only recently reported some structural characterization of ^{13}C GO films using nuclear magnetic resonance spectroscopy.[22]

The graphene oxide samples studied here were prepared by a modified Hummers method,[23] which results in a suspension of GO flakes in distilled water. Detailed descrip-

* To whom correspondence should be addressed. E-mail: mkhoyan@umn.edu.
† School of Applied and Engineering Physics, Cornell University.
‡ University of Minnesota.
§ Cornell Nanoscale Facility, Cornell University.
|| Rutgers University.

10.1021/nl8034256 CCC: $40.75
Published on Web 02/06/2009

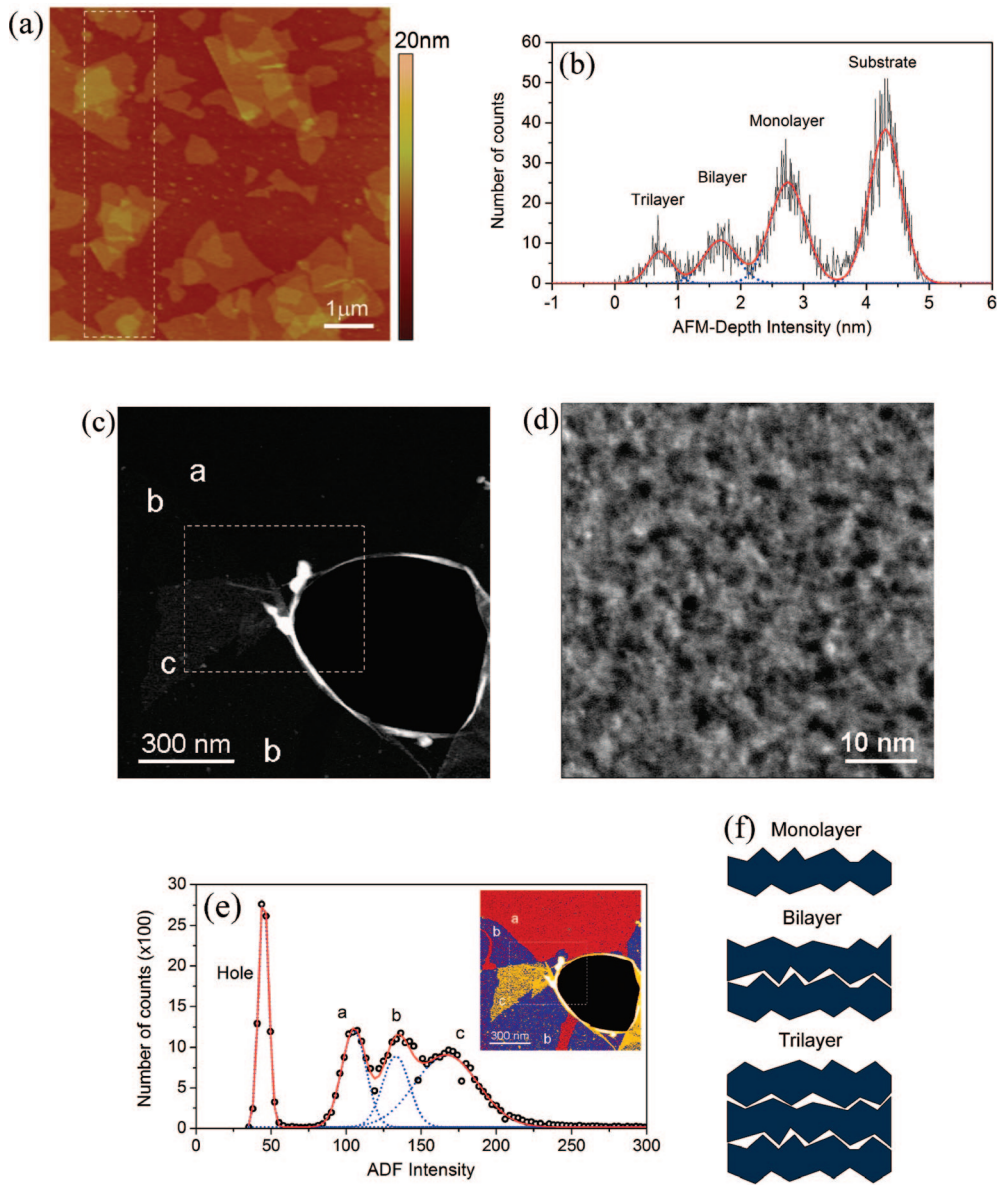

Figure 1. (a) AFM image of the GO films where mono-, bi-, and trilayers of GO films can be identified. (b) Histogram of the AFM-depth intensities obtained from dotted area of the image a. The histogram is fitted with a linear combination of four Gaussian functions representing each peak. (c) STEM-ADF image of the GO films where mono-, bi- and trilayers are labeled as a, b, and c, respectively. Round opening in the middle is a hole through the single film. (d) High-magnification ADF image of monolayer GO film. (e) Histogram of the ADF intensities obtained from dotted area of the image c with distinct intensities from mono-, bi-, trilayer films and hole. The intensity from the hole corresponds to the dark current of the ADF detector. The histogram is fitted with a linear superposition of four Gaussian functions representing each peak and peaks are labeled in accordance with the number of sheets as in panel c. The inset is the ADF image in c in colors emphasizing hole and different number of GO films. (f) Simple drawings illustrating monolayer and possible packing of bi- and trilayers.

tion of the preparation process can be found in Supporting Information of ref 6. Initial analysis of the GO sheets deposited on a SiO_2/Si substrate was conducted by atomic force microscopy (AFM) imaging and profiling. Several GO sheets consisting of mono-, bi-, and trilayers can be readily identified in the AFM image shown in Figure 1a. For quantitative analysis of flake height (or thickness), histograms of the AFM-depth profiles were obtained. The histogram obtained from the dotted region of the scan in panel a is shown in Figure 1b. The histogram was fitted with a linear superposition of four Gaussian curves to identify the peak positions and widths. It shows that the thickness of a single sheet is about 1.6 nm and the ratio of thicknesses of the mono-, bi-, and trilayers scale as 1:1.6:2.2 (with actual values being 1.6:2.6:3.6 nm) and surprisingly not as 1:2:3, which is also in agreement with a previous report by Jung et al.[24]

For the STEM study, GO flakes were deposited on standard holey-carbon-film-covered copper grids and loaded into the microscope. The experiments were carried out in the Cornell VG HB-501 100 kV STEM (for details, see Supporting Information). Before conducting any measurements, the GO samples were tested against electron-beam-induced damage and possible contamination, and no damage or contamination was observed for the STEM operational

conditions used during the main study. Composition and thickness sensitive ADF images were recorded in single-electron-counting mode for quantitative analysis. ADF image of the several layers of the GO suspended over a hole is shown in Figure 1c. While the mono, bi-, and trilayered films can be imaged, the signal from the single layer was found to be very weak as indicated by the fact that it is barely distinguishable from the hole in the middle of the image. However, a high-magnification ADF image taken from this single sheet reveals not only the sheet but also the variation of intensities within the image. Figure 1d is one such high-resolution image from a single layer GO. Strong variation of the ADF intensity in the single film suggests that the oxidation of the graphene is uniformly random throughout the sheet. Analysis of the ADF intensities from the dotted regions of Figure 1c reveals that the thicknesses of the mono-, bi-, and trilayers (relative to the intensity from the hole) scale as 1:1.5:2.0 (see Figure 1e), similar to the AFM results. The phenomenon can be explained by effective packing of the GO layers. The random covalent attachment of oxygen on the top and bottom surfaces creates a disordered graphene sheet and introduces roughness. The roughness of the sheets then allows effective packing of the multiple layers as schematically illustrated in Figure 1f, where oxygen atoms appear as protrusions. The observation of insensitivity of the FWHMs of the peaks in the AFM-histogram and their gradual increase in ADF-histogram with increasing number of sheets is additional confirmation of such packing. A critical observation from the AFM-depth profiles reveals that the GO sheet surface roughness is at least 0.6 nm. Since all known C−O bond lengths do not exceed 0.3 nm,[26] oxygen bonds alone cannot account for 0.6 nm height increase; therefore, the oxidation of graphene must be accompanied by undulations arising from lattice distortions in the original atomic structure of the graphene sheets.

For a better understanding of the high-resolution ADF-STEM images of the GO films, several images were simulated. Four potentially possible bonding sites for an oxygen atom on the honeycomb structure of graphene were considered and corresponding ADF images were simulated by applying Multislice computational method[27,28] using the code developed by Kirkland[29] (see Supporting Information for details). The results of simulations are presented in Figure 2. ADF images of graphene with three double bonds of oxygen to carbon atoms and one with a single bond are shown in Figure 2a−d, respectively. An ADF image of a graphene with oxygen atoms attached to both side of the sheet was simulated and the resulting image is shown in Figure 2e. Here oxygen atoms were considered to be randomly attached to the carbon atoms from both sides of the graphene sheet with two restrictions; the ratio of oxygen to carbon atoms was kept close to the experimentally measured value and each carbon atom was bonded to only one oxygen atom. As can be seen from simulated ADF image in Figure 2e, the presence of oxygen on both surfaces of the graphene is sufficient for creating strong intensity variations observed experimentally (see Figure 1d) and for the loss of the visibility of the underlying periodicity of graphene. These

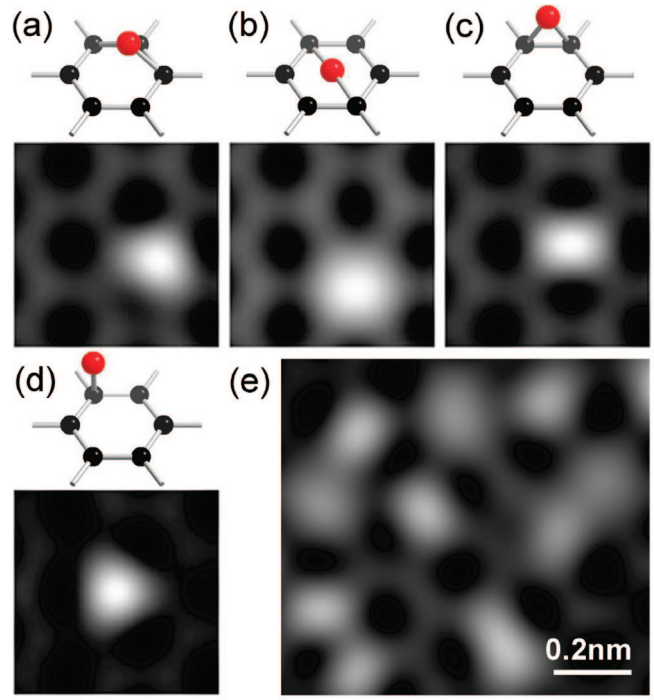

Figure 2. Simulated STEM-ADF images of graphene with oxygen atoms attached to the surface. (a−d) Images represent possible cases of oxygen atom bonded to the honeycomb of the graphene. The ball-stick models at the top illustrate the structures. (e) Simulated image of the graphene with oxygen atoms randomly connected to both surfaces of the graphene. Here 1:5 ratio of oxygen to carbon atoms were considered. Images were simulated using 2 Å STEM probe. All images are individually scaled to fill the available grayscale.

simulations also suggest that not only can single oxygen atoms be directly imaged on graphene substrate using STEM-ADF detector but the actual sites of the honeycomb to which the atom is attached can also be identified. It should be noted here that additional study is required to determine which oxygen bonding sites from these four are favorable in GO.

To study the electronic structure of GO films, core-level EELS spectra of C and O K-edges, which represent the respective 2p partial density-of-states above the Fermi level, were measured from several single GO sheets. Figure 3a shows the C K-edge recorded from GO film in Figure 1a and for comparison plotted with C K-edge spectra from amorphous-carbon (a-C) and graphite.[30] A spectrum of the O K-edge measured from the same sheet is presented in Figure 3b and compared with corresponding spectrum in a-SiO_2. The fine structure of the C K-edge in GO shows considerable differences relative to those in graphite and a-C.[13,31] However, it also indicates the presence of σ^* peak with energy close to that in graphite (peak labeled B in Figure 3a). The positions of identifiable peaks in a C K-edge in all three materials summarized in Table 1 suggest that both sp^2 and sp^3 bonds are present in the GO. To enhance the fine structure in C K-edge, the STEM probe function was removed from the data and the resulting spectrum is shown in Figure 3c. The fine structure of O K-edge, which lacks distinct features, indicates the absence of periodicity for the oxygen atoms in the film.[13] Since there is no existing carbon-

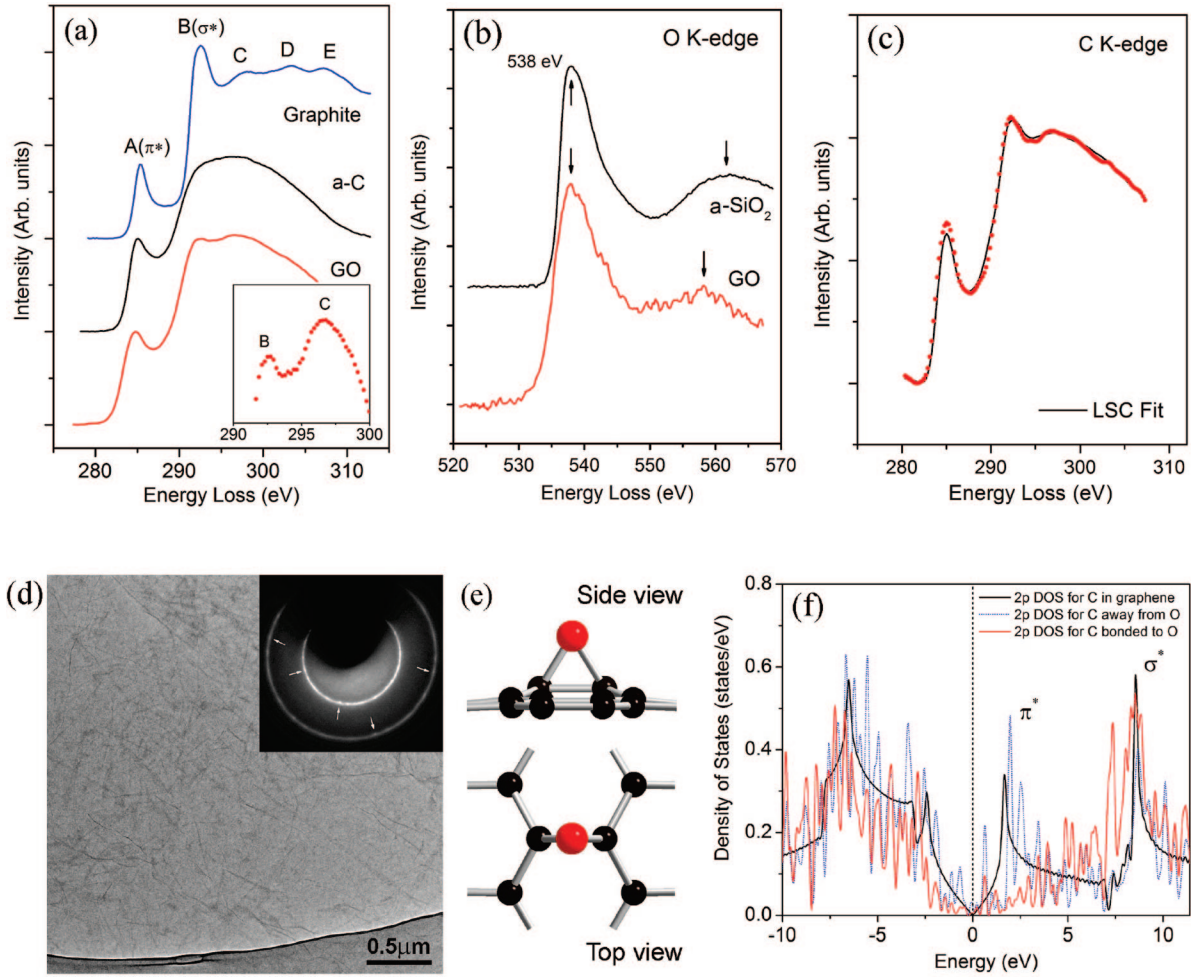

Figure 3. Core-loss EELS spectra of (a) C K-edge and (b) O K-edge from the GO film. Both spectra were recorded from the film labeled a in Figure 1c. The spectrum of C K-edge is presented in comparison with C K-edges measured in graphite and a-C recorded using the same STEM and similar electron-optical conditions. The peaks of the fine structure are labeled A−E. The inset shows section of the spectrum from GO for better visibility of the positions of the peaks B (or σ^*) and C. The O K-edge is presented in comparison with O K-edge in a-SiO_2 also recorded using the same STEM and similar electron-optical conditions. (c) The spectrum of the C K-edge in GO film and its best fit after removal of STEM probe function. (d) Conventional TEM image of many layers of GO films suspended over the hole in TEM grid. The inset is the diffraction pattern from this multilayer. The arrows indicate some of the bright spots on the diffraction rings. Dark area on the top is the shadow of "beam stop" used to block the central spot. Image and diffraction pattern are obtained using FEI Technai T20 STEM/TEM operating at 200 keV. (e) Ab initio calculated atomic structure of the graphene sheet with single O atom bonded to two adjacent C atoms. (f) Carbon 2p partial DOS calculated for graphene and for C atom of graphene bonded to O and one that is far away from O.

Table 1. Positions of the Peaks in C K-edge Recorded from Graphite, a-C, and GO Films[a]

	A (π^*)	B (σ^*)	C	D	E
graphite	285.4	292.5	298.2	303.4	307.2
a-C	284.7		~296		
GO	284.8	292.6	296.7	302.9	

[a] For identification of the peaks labeled A−E, see Figure 3. All energies are in (eV).

oxide in solid form, the O K-edge spectrum from GO sheets was compared with O K-edge of a-SiO_2, which also has an initial peak at 538 eV and an extended broad second peak at about 560 eV.[33] Strong similarities between the two are noticeable.[34] These results are in agreement with ADF imaging showing random attachment of oxygen atoms on graphene sites during oxidation. Integrated intensities of the C and O K-edges give a 1:5 ratio for number of O to C atoms.

To evaluate the amount of sp^2- and sp^3-C bonds in GO films, the spectrum of the C K-edge was fitted to a linear superposition of two spectra, C K-edge from graphite and a-C. After normalizing both spectra, a linear least-squares curve fitting algorithm[32] was applied to determine coefficients α_1 and α_2 of the fitting function:

$$I(E) = \alpha_1 I^{g}(E) + \alpha_2 I^{am}(E) \quad (1)$$

Here $I^{g}(E)$ and $I^{am}(E)$ are the spectra from graphite and a-C, respectively. For the C K-edge measured from a single GO film (see in Figure 3c), the best fit occurs at $\alpha_1 = 0.15$ and $\alpha_2 = 0.85$, indicating that only 15% of the carbon atoms inside the films are graphite-like, and 85% behave amorphous-carbon-like. This suggest that the atomic structure of GO films should resemble a mostly amorphous 2D sheet of carbon atoms with some of them also bonded to oxygen, rather than an ideal sheet of graphene with surface oxidation.

Electron diffraction patterns, obtained from several layers of these GO films and one presented in Figure 3d, support this structural model. The pattern is dominated by diffraction rings occurring due to the amorphous nature of the sample. It also shows the presence of some bright spots on the rings which is a indication of some crystallinity in the films and is consistent with having 15% residual graphene-like structure in the films. The portion of sp^3 bonds in a-C used here, based on EELS data analysis,[13,35,36] is estimated to be about 45%, which leads to an actual amount of carbon sp^3 bonds in the GO to be about 40%. The partial amorphization of the GO can be explained by modification of the original sp^2 bonds of carbon atoms of the graphene into sp^3 bonds via bonding with oxygen and in the process moving carbon atoms from their original sites to accommodate the off-plane sp^3 bonds. To confirm this, detailed ab initio density functional theory (DFT) based calculations were performed.

A series of DFT calculations using a plane wave pseudopotential approach were performed for two cases, pristine graphene and a graphene supercell with a single oxygen atom. The technical details of the calculations can be found in the Methods section in Supporting Information. The results of structural relaxation calculations for the equilibrium configuration of the atoms when an O atom is present shows (i) the two carbon atoms bonded to the oxygen atom are pulled above the graphene plane as shown in Figure 3e (this configuration is fairly stable with an absorption energy of −3.12 eV) and (ii) the bond length between these two carbon atoms expands from 1.407 Å in graphene to 1.514 Å, which is close to 1.54 Å sp^3 bond length in diamond. Such bond expansion in the presence of oxygen has been previously predicted for epoxy groups on graphene.[37,38] This may explain the 0.6 nm surface roughness of the films detected by AFM scans. A simple estimate calculating the probability of finding a carbon atom in the sheet that is not oxidized and has only unoxidized neighboring carbons (necessary for sp^2-like bond) shows that O/C ratio of 1:5 is more than sufficient to transform 40% of the original carbon bonds in graphene into sp^3 bonds.

The calculated partial, 2p, density of states (DOS) for pristine graphene and graphene with an epoxy group is shown in Figure 3f. For graphene, the calculated energy difference between the π^* and σ^* peaks was 6.89 eV, which is in good agreement with the measured energy difference in graphite (7.1 eV). In the case of the graphene supercell with an epoxy group, the presence of the oxygen atom distorts the lattice, breaks the symmetry of the system, and induces a band gap. The local DOS for a C atom far from the O (about 0.65 nm) is similar to that found in pristine graphene. However, the DOS of the C atoms bonded to O is significantly different. Here the π^* peak is absent for these C atoms and the σ^* is broadened in good correlation with the sp^3 bond fingerprint measured in diamond.[13]

The low-loss EELS spectrum, which is a direct measure of the dielectric response of the film to the external electromagnetic excitation, was recorded from a single GO sheet and is presented in Figure 4. When compared with corresponding spectra from graphite and a-C, significantly

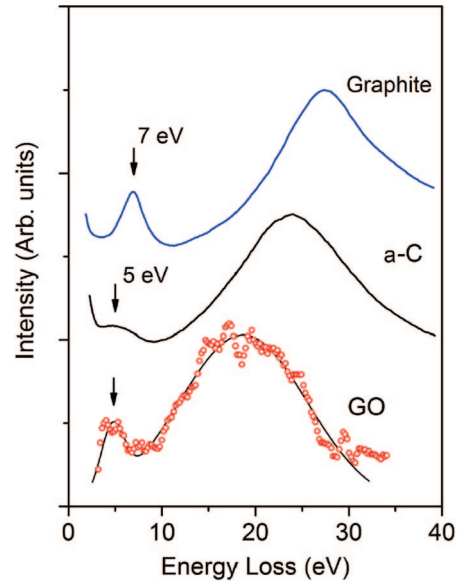

Figure 4. Low-loss EELS spectrum showing plasmon excitations in GO films. The spectrum is recorded from the film labeled a in Figure 1c. It is presented in comparison with corresponding spectra from graphite and a-C recorded using the same STEM and similar electron-optical conditions.

lower energy plasma excitations are observed. While in graphite and a-C, the peaks of bulk plasma-loss (combination of π^* and σ^* electronic excitations) are at 27 and 24 eV, respectively, in GO films it is much lower at 19 eV.[30] The low-energy plasma excitations of the π^* electrons in GO however occurs at 5 eV, similar to that in a-C. Since the thickness of the film is only 1−2 nm thick, the origin of 19 eV main plasma resonance in GO films can be fully understood only when a full quantum mechanical description is applied. For specimens with thickness smaller than 5 nm, it is well known that surface plasma excitations are often the dominating mechanisms for energy loss.[39,40] But for specimens a few atomic layers thick, such a macroscopic description may not be sufficient. A very recent study by Eberlein et al. that combined EELS measurements with first principle calculations found that the plasmon modes of pure graphene are significantly red-shifted from those found in graphite.[21,41] They measured the main $\pi^* + \sigma^*$ plasma peak at 14.6 eV and a π^* peak at 4.7 eV. This suggests that in GO the plasma excitations could be related to those in graphene but with substantial blue-shift occurring due to presence of the oxygen and increased number of sp^3 bonds.

In conclusion, electron energy loss spectroscopy combined with STEM-ADF imaging and AFM-depth profiling shows that graphene oxide films have substantially different density-of-states and resonance electron plasma excitation energy than those in graphene and a-C. It also indicates that oxygen atoms attach to graphene sites randomly and convert sp^2 carbon bonds in graphene to sp^3 bonds. While the structural modifications of graphene are dependent on the oxidation level, the results show that a ratio of 1:5 oxygen to carbon atoms is sufficient to transform the measured 40% of the carbon bonds into sp^3 bonds. As a consequence, the atomic structure of oxidized

graphene is highly distorted, becoming a semiamorphous solid carbon oxide with undulations resulting in a surface roughness of about 0.6 nm. These results are also supported by our ab initio calculations. Our results provide new insight into the structure of graphene oxide and indicate that in addition to the removal of oxygen, structural ordering of the remaining graphene sheets is necessary if high mobilities from reduced graphene oxide devices are to be achieved.

Acknowledgment. This work is supported primarily by the Nanoscale Science and Engineering Initiative of the NSF EEC-0117770 and NYSTAR C020071 through Cornell University. The sample preparation facilities and STEM are supported by NSF through the Cornell Center of Materials Research DMR 9632275. Density functional calculations were performed on the Intel cluster at the Cornell Nanoscale Facility. A.W.C. would like to acknowledge financial support of Intel through Cornell Engineering Learning Initiatives and D.A.S. the support of Cornell Nanoscale Science and Technology Facility. Authors would also like to acknowledge technical support of M. Thomas with VG STEM, L.F. Kourkoutis and J. Grazul with Technai STEM/TEM, G. Fanchini for his help in preparing the initial GO suspensions and NSF CAREER Award ECS 0543867 to M.C.

Supporting Information Available: Detailed experimental and theoretical methods. Additional experimental results and simulations. This material is available free of charge via the Internet at http://pubs.acs.org.

References

(1) Stankovich, S.; Dikin, D. A.; Dommett, G. H. B.; Kohlhaas, K. M.; Zimney, E. J.; Stach, E. A.; Piner, R. D.; Nguyen, S. T.; Ruoff, R. S. *Nature* **2006**, *442*, 282.
(2) Dikin, D. A.; Stankovich, S.; Zimney, E. J.; Piner, R. D.; Dommett, G. H. B.; Evmenenko, G.; Nguyen, S. T.; Ruoff, R. S. *Nature* **2007**, *448*, 457.
(3) Stankovich, S.; Piner, R. D.; Chen, X.; Wu, N.; Nguyen, S. T.; Ruoff, R. S. *J. Mater. Chem.* **2006**, *16*, 155.
(4) Stankovich, S.; Piner, R.; Nguyen, S. T.; Ruoff, R. S. *Carbon* **2006**, *44*, 3342.
(5) Watcharotone, S.; Dikin, D. A.; Stankovich, S.; Piner, R.; Jung, I.; Dommett, G. H. B.; Evmenenko, G.; Wu, S.-E.; Chen, S.-F.; Liu, C.-P.; Nguyen, S. T.; Ruoff, R. S. *Nano Lett.* **2007**, *7*, 1888.
(6) Eda, G.; Fanchini, G.; Chhowalla, M. *Nat. Nanotechnol.* **2008**, *3*, 270.
(7) Eda, G.; Lin, Y-Y.; Miller, S.; Chen, C.-W.; Su, W.-F.; Chhowalla, M. *Appl. Phys. Lett.* **2008**, *92*, 233305.
(8) Gomez-Navarro, C.; Weitz, R. T.; Bittner, A. M.; Scolari, M.; Mews, A.; Burghard, M.; Kern, K. *Nano Lett.* **2007**, *7*, 3499.
(9) Ramanathan, T.; Abdala, A. A.; Stankovich, S.; Dikin, D. A.; Herrera-Alonso, M.; Piner, R. D.; Adamson, D. H.; Schniepp, H. C.; Chen, X.; Ruoff, R. S.; Nguyen, S. T.; Aksay, I. A.; Prud'Homme, R. K.; Brinson, L. C. *Nat. Nanotechnol.* **2008**, *3*, 327.
(10) Becerril, H. A.; Mao, J.; Liu, Z.; Stoltenberg, R. M.; Bao, Z.; Chen, Y. *ACS Nano* **2008**, *2*, 463.
(11) Wu, J.; Becerril, H. A.; Bao, Z.; Liu, Z.; Chen, Y.; Peumans, P. *Appl. Phys. Lett.* **2008**, *92*, 263302.
(12) Wang, S.; Chia, P.-J.; Chua, L.-L.; Zhao, L.-H.; Png, R.-Q.; Sivaramakrishnan, S.; Zhou, M.; Goh, R. G.-S.; Friend, R. H.; Wee, A. T.-S.; Ho, P. K.-H. *Adv. Mater.* **2008**, *20*, 3440.
(13) Egerton, R. F. *Electron Energy Loss Spectroscopy in the Electron Microscope*; Plenum Press: New York; 1996.
(14) Muller, D. A.; Singh, S.; Silcox, J. *Phys. Rev. B* **1998**, *57*, 8181.
(15) Mkhoyan, K. A.; Silcox, J.; Alldredge, E. S.; Ashcroft, N. W.; Lu, H.; Schaff, W. J.; Eastman, L. F. *Appl. Phys. Lett.* **2003**, *82*, 1407.
(16) Daniels, J.; Festenberg, C. V.; Raether, H.; Zeppenfeld, K. *Springer Tracts in Modern Physics*; Ḧ ohler, G., Ed.; Springer-Verlag: Berlin, 1970; Vol. 54, p 77.
(17) Meyer, J. C.; Geim, A. K.; Katsnelson, M. I.; Novoselov, K. S.; Booth, T. J.; Roth, S. *Nature* **2007**, *446*, 60.
(18) Meyer, J. C.; Girit, C. O.; Crommie, M. F.; Zettl, A. *Nature* **2008**, *454*, 319.
(19) Wang, G.; Yang, J.; Park, J.; Gou, X.; Wang, B.; Liu, H.; Yao, J. *J. Phys. Chem. C* **2008**, *112*, 8192.
(20) Meyer, J. C.; Kisielowski, C.; Erni, R.; Rossell, M. D.; Crommie, M. F.; Zettl, A. *Nano Lett.* **2008**, *8*, 3582.
(21) Gass, M. H.; Bangert, U.; Bleloch, A. L.; Wang, P.; Nair, R. R.; Geim, A. K. *Nat. Nanotechnol.* **2008**, *3*, 676.
(22) Cai, W.; Piner, R. D.; Stadermann, F. J.; Park, S.; Shaibat, M. A.; Ishii, Y.; Yang, D.; Velamakanni, A.; An, S. J.; Stoller, M.; An, J.; Chen, D.; Ruoff, R. S. *Science* **2008**, *321*, 1815.
(23) Hirata, M.; Gotou, T.; Horiuchi, S.; Fujiwara, M.; Ohba, M. *Carbon* **2004**, *42*, 2929.
(24) Jung, I.; Pelton, M.; Piner, R.; Dikin, D. A.; Stankovich, S.; Watcharotone, S.; Hausner, M.; Ruoff, R. S. *Nano Lett.* **2007**, *7*, 3569.
(25) (a) Mkhoyan, K. A. Ph.D. Thesis, Cornell University, Ithaca, NY, 2004. (b) Mkhoyan, K. A.; Kirkland, E. J.; Silcox, J.; Alldredge, E. S. *J. Appl. Phys.* **2004**, *96*, 738.
(26) *CRC Handbook of Chemistry and Physics*, 85th edition; Lide, D. R., Ed.; Plenum: New York, 2004.
(27) Cowley, J. M.; Moodie, A. F. *Acta Crystallogr.* **1957**, *10*, 609.
(28) (a) Kirkland, E. J.; Loane, R. F.; Silcox, J. *Ultramicroscopy* **1987**, *23*, 77. (b) Loane, R. F.; Xu, P.; Silcox, J. *Acta. Cryst.* **1991**, *A47*, 267.
(29) Kirkland, E. J. *Advanced Computing in Electron Microscopy*; Plenum Press, New York, 1998.
(30) It should be noted here that in hexagonal crystals like graphite the fine structure of the core-edges like C K-edge as well as low-loss excitations are sensitive to the orientation of the crystal relative to the incident electron beam and scattered beam collection geometry. All the core-edges and low-loss spectra from graphite and GO films presented here are recorded with electron beam oriented parallel to *c*-axis and perpendicular to the sheets and with similar collection geometry.
(31) Batson, P. E. *Phys. Rev. B* **1993**, *48*, 2608.
(32) Press, W. H.; Teukolsky, S. A.; Vetterling, W. T.; Flannery, B. P. *Numerical Recipes in C++*; Cambridge University Press: Cambridge, England, 2003.
(33) Muller, D. A.; Sorsch, T.; Moccio, S.; Baumann, F. H.; Evans-Lutterodt, K.; Timp, G. *Nature* **1999**, *399*, 758.
(34) The actual position of the peaks of O K-edge in GO films are strong initial peak is at 538 eV and extended broader peak is at about 558 eV.
(35) Berger, S. D.; McKenzie, D. R.; Martin, P. J. *Philos. Mag. Lett.* **1988**, *57*, 285.
(36) Cuomo, J. J.; Doyle, J. P.; Bruley, J.; Liu, J. C. *Appl. Phys. Lett.* **1991**, *58*, 466.
(37) Li, J.-L.; Kudin, K. N.; McAllister, M. J.; Prudhomme, R. K.; Aksay, I. A.; Car, R. *Phys. Rev. Lett.* **2006**, *96*, 176101.
(38) Schniepp, H. C.; Li, J-L.; McAllister, M. J.; Sai, H.; Herrera-Alonso, M.; Adamson, D. H.; Prudhomme, R. K.; Car, R.; Saville, D. A.; Aksay, I. A. *J. Phys. Chem. B* **2006**, *110*, 8535.
(39) Raether, H. Excitations of Plasmons and Interband Transitions by Electrons. In *Springer Tracts in Modern Physics*; Ḧ ohler, G., Ed.; Springer-Verlag: Berlin, 1980; Vol. 88.
(40) Mkhoyan, K. A.; Babinec, T.; Maccagnano, S. E.; Kirkland, E. J.; Silcox, J. *Ultramicroscopy* **2007**, *107*, 345.
(41) Eberlein, T.; Bangert, U.; Nair, R. R.; Jones, R.; Gass, M.; Bleloch, A. L.; Novoselov, K. S.; Geim, A.; Briddon, P. R. *Phys. Rev. B* **2008**, *77*, 233406.

NL8034256